Vol. 157: 21–37, 1997 | MARINE ECOLOGY PROGRESS SERIES Mar Ecol Prog Ser | Published October 16

Dissolved organic matter in a temperate embayment affected by coastal upwelling

M. D. Doval*, X. A. Álvarez-Salgado, Fiz F. Pérez

Instituto de Investigacións Mariñas, C.S.I.C., Eduardo Cabello, 6, E-36208 Vigo, Spain

ABSTRACT: From September 1994 to September 1995 a time-series station in the Ría de Vigo (NW Spain) was monitored fortnightly. Dissolved organic carbon (DOC) was analysed by high temperature catalytic oxidation. Dissolved organic nitrogen (DON) was determined by the Kjeldahl method, after removal of inorganic nitrogen from the sample. The time courses of DOC and DON changes were parallel. The average C/N molar ratio of dissolved organic matter (DOM) was ~15. DOM was strongly influenced by physical and biological processes. During the upwelling season, the entry of DOM-poor Eastern North Atlantic Central Water (ENACW) controlled DOM levels in subsurface waters. Biologically produced DOM excess in surface waters was uncoupled with chlorophyll *a* on a daily time-scale. A tentative partitioning of DOM during the upwelling season has been inferred from mixing of oceanic and freshwater endmembers. The refractory pool, ~70% of total DOC in surface water, was carried by upwelled ENACW (60%, 10% of which was semi-refractory) and continental water (10%). Net production of semi-labile DOC occurred in the bottom layer (~10 µM C). The average DOC excess in surface waters compared to bottom waters was 21 µM C ,with a C/N molar ratio of 12. The excess was a mixture of labile and semi-labile material with a recycling time >5 d, which represented ~23 and ~13% of the net primary production for C and N respectively. The average DOM excess/[POM (particulate organic matter) + DOM excess] ratio in surface waters was ~0.4 and ~0.3 for C and N respectively, indicating that POM was the most important pool of organic matter net produced in the inner ría. During the downwelling season DOM was balanced by the external inputs and the DOM excess in surface waters was due to the freshwater contribution.

KEY WORDS: DOC · DON · Upwelling · Downwelling · Ría de Vigo · NW Spain

INTRODUCTION

Recent studies indicate that a considerable fraction of the dissolved organic matter (DOM) pool in seasonal thermocline waters is highly labile ($t_{1/2}$ ≈ hours to days) and/or semi-labile ($t_{1/2}$ ≈ months), and is generated *in situ* by biological processes (Kirchman et al. 1993, Carlson & Ducklow 1995). The few estimates of this fraction are in the range of 1 to 50% of the total dissolved organic carbon, DOC (Chen & Wangersky 1996). The highly labile DOM fuels the 'microbial loop' (Azam et al. 1983, Jumars et al. 1989, Kirchman et al. 1991). The semi-labile DOM, which escapes utilisation in the microbial food web, accumulates in seasonal thermocline waters and it is exported to the deep ocean mainly during winter mixing. Annual downward transport of semi-labile DOC can be greater than the particulate organic carbon (POC) flux in oligotrophic areas (Copin-Montégut & Avril 1993, Carlson et al. 1994, Murray et al. 1994, Lefèvre et al. 1996). Consequently, highly labile and semi-labile DOM play a major role in the regenerated and new production of marine systems, and need to be considered in biogeochemical models (Kirchman et al. 1993, Bronk et al. 1994). DOM lability can be approached through the C/N ratio (Cherrier et al. 1996). In this sense, observed seasonal accumulation of carbon-rich DOM (high C/N ratio) can be due to reduced bacterial activity in inorganic nitrogen depleted waters during the summer (Williams 1995).

The most intense production of organic matter in the ocean occurs in the coastal zone. Although it comprises

*E-mail: marylo@iim.csic.es

only ca 8% of the total surface area of the ocean, the coastal zone accounts for 18 to 28% of ocean primary production because of large atmospheric, riverine and, most importantly, ocean inputs (Wollast 1991, 1993). Enhanced primary production increases fluxes between carbon pools (ΣCO_2, POC and DOC) through biogeochemical processes. Ocean inputs are greatly intensified in upwelling areas (Walsh 1991).

The NW Africa upwelling system extends from 10° to 44° N (Wooster et al. 1976). The northern boundary, on the western coast of the Iberian Peninsula (42° to 43° N), is occupied by the Rías Baixas. These are 4 large coastal embayments (2.7 to 4.3 km^3), freely connected (open to the oceanic influence) with the adjacent shelf. They gradually deepen and widen towards the mouth, thus favouring export (Odum et al. 1979).

From April to October (the upwelling season), northerly winds cause Eastern North Atlantic Central Water (ENACW) to upwell over the shelf with a 10 to 15 d periodicity (Blanton et al. 1987, Álvarez-Salgado et al. 1993). Nutrient-rich ENACW enters the rías by means of the enhanced positive residual circulation (Prego & Fraga 1992, Rosón et al. 1997). The rías allow increased residence time of upwelled water in the photic layer and, in comparison with adjacent shelf surface waters, enhance the influence of solar heating on thermocline formation and of phytoplankton on nutrient uptake (Álvarez-Salgado et al. 1996b). Periodic nutrient pulses induce a succession of new production maxima, supported mainly by external nitrate. The average ratio of new to total production (f_{ratio}) is very high (~0.5 to 0.6) during the upwelling season (Ríos 1992, Moncoiffé 1995, Álvarez-Salgado et al. 1996a). However, part of the inflowing nitrate comes from shelf mineralisation of organic matter part of which was exported from the rías (Fraga 1981, Prego 1994, Álvarez-Salgado et al. 1996a, 1997). The mean annual new production is about 800 mg C m^{-2} d^{-1} (Prego 1993a). It increases to 1200–1500 mg C m^{-2} d^{-1} during the upwelling season (Fraga 1976, Moncoiffé 1995, Álvarez-Salgado et al. 1996a) and to >3000 mg C m^{-2} d^{-1} during upwelling pulses, when the f_{ratio} is ~1 (Álvarez-Salgado et al. 1996a).

During the autumn transition from northerly to southerly winds (October–November), strong reversal of the positive circulation occurs, displacing the downwelling front on the shelf towards the rías. In this situation, the ammonium concentration in the water column is increased because of net release from the sediment-water interface, and high sedimentation rates result from intense transport of particulate matter to the lower layer (Álvarez-Salgado et al. 1996b).

From November to February (the downwelling season), southerly winds prevail. During the winter, positive residual circulation is resumed due to strong continental inputs to the rías (Rosón et al. 1991, Prego & Fraga 1992, Ríos et al. 1992), which keep the downwelling front on the shelf Haline stratification prevents vertical homogenisation resulting from temperature inversion. Mixing of nutrient-rich continental and shelf waters characterises nutrient distributions in the surface layer. Contrary to the behaviour during the upwelling season, nutrient concentrations in bottom waters are lower than in the surface (Fraga 1967, Mouriño et al. 1984, Prego 1993b, 1994). The maximum nutrient excess occurs by January. The average excess is ~4 µmol kg^{-1} for dissolved inorganic nitrogen (DIN) at the time-series station, in the middle of the Ría de Vigo (Nogueira et al. 1997a).

The transition from southerly to northerly winds (February–March) is accompanied by a sharp decrease in surface nutrient concentrations (Nogueira et al. 1997a), characteristic of spring bloom conditions. In summary, the balance between river discharge and shelf wind-stress determines the residual flows and, ultimately, the nutrient biogeochemistry in the rías. These coastal inlets behave like an extension of the shelf during the upwelling season and like a partially mixed estuary during the downwelling season (Doval et al. 1997b).

In spite of our knowledge on nutrient dynamics in the Rías Baixas, the key contribution of organic matter, particularly DOM, towards balancing nutrient budgets (Álvarez-Salgado et al. 1996a, b) has not been rigorously assessed. Dissolved and particulate organic nitrogen (DON and PON) (Fraga 1960, 1967, Fraga & Vives 1961), total organic carbon and nitrogen (TOC and TON) (Prego 1993a, 1994), and POC and PON (Figueiras & Niell 1987, Ríos 1992, Alvarez-Salgado et al. 1996a, b) distributions have been produced in the rías. However, this is the first time that all carbon and nitrogen pools have been quantified simultaneously. The present work focuses on the annual cycle of DOC and DON in the Ría de Vigo. The influence of meteorologically forced hydrography and biogeochemistry on changes in DOM is examined.

MATERIALS AND METHODS

The time-series station, in the main channel of the Ría de Vigo (42° 14.5' N, 8° 45.8' W), was visited twice a week beginning in 1987 (Fig. 1). The sampling site, 45 m depth, is sensitive to both continental and ocean influences and has 2 advantages over a station on the shelf: (1) it is easily accessible and well protected against inclement weather conditions in wintertime; and (2) circulation can be successfully characterised using a 2-dimensional approach. Abundant hydrographic data from the time-series station (salinity,

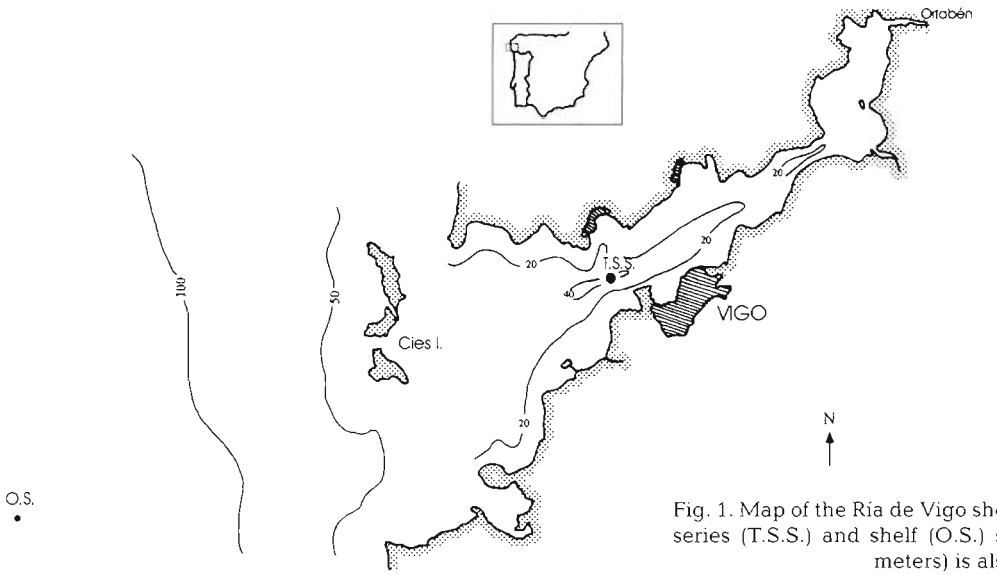

Fig. 1. Map of the Ría de Vigo showing the location of the time series (T.S.S.) and shelf (O.S.) stations. The bathymetry (in meters) is also shown

temperature, nutrients and chlorophyll *a*) are essential for an understanding of the nutrient dynamics of the rías on both seasonal and short time scales (Figueiras et al. 1994, Nogueira et al. 1997a, b, in press). From September 1994 to September 1995 additional samples for DOC, DON, POC, PON, pH and alkalinity were taken at 2 wk intervals at depths of 1, 15 and 40 m at the time-series station. The survey numbers (from 9 to 34) indicate the date of sampling In addition, samples were taken in a shelf station (O.S.) to estimate the DOM concentration of upwelled ENACW.

Analytical details. A Seabird Electronics 25-01 CTD (conductivity/temperature/depth profiler) was dipped before the bottles were cast. Samples were drawn from 3 depths (0, 15 and 40 m) with 5 l Niskin bottles. Salinity was determined from conductivity measurements with an AUTOSAL 8400 A (UNESCO 1985) in order to calibrate the probe. Temperature was tested with reversing thermometers.

Samples for nutrient analyses were collected in polyethylene containers. They were frozen to −20°C until analysis in the laboratory using standard segmented flow analysis (SFA) procedures (Hansen & Grashoff 1983, Mouriño & Fraga 1985, Álvarez-Salgado et al. 1992). Chlorophyll *a* was determined fluorometrically, with a Turner Designs 10000R fluorometer. pH (National Bureau of Standards, NBS) was measured potentiometrically according to Pérez & Fraga (1987a). Alkalinity was determined by acid titration to pH 4.4 following Pérez & Fraga (1987b). Dissolved inorganic carbon (ΣCO_2) was calculated by substituting pH and alkalinity in the carbonic acid systems equations, using the constants proposed by Mehrbach et al. (1973) and in agreement with Takahashi et al. (1993).

A volume of 1 l of sample was filtered through an oilless vacuum filtration system. POC and PON were collected on Whatman GF/F filters, which were dried on silica gel and frozen to −20°C until analysis in the laboratory. Measurements were carried out with a Perkin Elmer 2400 CHN analyser. Combustion to CO_2 and NO_x was performed at 900°C and reduction of NO_x to N_2 at 640°C. Aliquots of the filtrate were taken for DOC and DON analyses.

DOC determination was performed by high temperature catalytic oxidation (HTCO) with a commercial Shimadzu TOC-5000. The combustion quartz tube was filled with a 0.5% Pt on Al_2O_3 catalyst. Three to 5 replicate injections of 200 µl were performed per sample. The concentration of DOC was determined by subtracting the average peak area from the instrument blank area and dividing by the slope of the standard curve (Thomas et al. 1995). The instrument blank is the system blank plus the filtration blank. The system blank was determined by subtracting the DOC in UV-Milli-Q from the total blank. Measurements made with the high sensitivity catalyst (Pt on silica wool) produced values < 2 µM C for fresh UV-Milli-Q water. The filtration blank was determined by filtering UV-Milli-Q water through the filtration system. The filtration blank was ~5 µM C. Before sample analyses, the catalyst was washed by injecting UV-Milli-Q, for at least 12 h, until the system blank was low and stable. The system blank was < 8 µM C; when it was higher, we washed or even replaced the catalyst. The system was standardised with potassium hydrogen phthalate (KHP). The coefficient of variation (CV) of the peak area for the 3 to 5 replicates of each sample was ~1%. We participated in the international intercalibration exercise conducted by J. Sharp (Univ. of Delaware), obtaining

satisfactory results (within ±10%; J. Sharp pers. comm.).

DON was directly measured by an updated Kjeldahl method (Doval et al. 1997a). A volume of 100 ml of sample was introduced into a 300 ml Pyrex Kjeldahl flask. To eliminate ammonium, 1 ml of 0.5 N NaOH was added and the solution was boiled until the sample was reduced by half. Next, 10 ml of H_2SO_4-$FeSO_4$ reagent was added to concentrate the sample and remove nitrogen oxides. The heating must be continued to convert DON to ammonium in acid medium. The residue was diluted with UV-Milli-Q water and carried to a distillation device, where 20 ml of 33% NaOH was added and the resulting ammonia was co-distilled with water vapour until 20 ml was collected over 5 ml of 10^{-3} M HCl. Finally, ammonium concentration on the distillate, which is directly related to DON in the sample, was determined with the SFA system. The most common biochemicals and most of the identified major constituents of seawater DON are accurately measured (recovery ≥95%) with this method, except for antipyrine (73%). The average blank was ~2 µM N. We analysed duplicate seawater samples, the CV being ~5%.

Meteorological and hydrographic indices. The upwelling index (I_w) is a gross estimation of the flow of upwelled water per kilometre of coast. According to Wooster et al. (1976):

$$I_w = \frac{\rho_a \cdot C \cdot |\bar{V}|}{f \cdot \rho_w} V_N \quad (1)$$

where ρ_a is the density of air, 1.2 kg m^{-3} at 15°C; C is an empirical drag coefficient (dimensionless), 1.3×10^{-3}; f is the Coriolis parameter, 9.9×10^{-5} s^{-1} at 43° latitude; ρ_w is the density of seawater, 1025 kg m^{-3}; $|\bar{V}|$ is wind speed and V_N is the north component of wind speed. The upwelling index was calculated using daily averaged geostrophic winds deduced from surface pressure charts following Bakun (1973). Negative values indicate downwelling. $<I_w>$ is the average I_w from the current day to 2 d before, which correlates better with the vertical displacement of the isopycnals, due to the inertia of coastal circulation to wind-stress (Rosón et al. 1997).

Continental runoff, Q_R, was estimated as the sum of a function of precipitation in the drainage basin, ~480 km^2 (Ríos et al. 1992), and the flow from the river Oitaben, regulated by the Eiras reservoir. $<Q_R>$ was calculated by averaging the daily flows from the current date to 4 d before. This was because the flushing time of the inner ría up to the time-series station is ~5 d, based on water flows calculated by Ríos (1992).

The Brunt-Väisälä frequency (Millard at al. 1990) is commonly used for evaluating the stability of the water column, $N^2 = (g/\rho)(\partial\rho/\partial z)$, where g is gravity, ρ is density and z is depth. The average N^2 integrated over the water column ($\overline{N^2}$) can be calculated as:

$$\overline{N^2} = \frac{g}{Z} \cdot \ln\left(\frac{\rho_b}{\rho_s}\right) \quad (2)$$

where Z is water depth (45 m), ρ_s is surface density, and ρ_b is bottom density.

Linear regression. The best fit between any pair of dependent (Y) and independent (X) variables was obtained by minimising

$$\sum_i \left[\left(X_i - \hat{X}_i\right)^{w_X} \left(Y_i - \hat{Y}_i\right)^{w_Y} \right]^2 \quad (3)$$

where w_X and w_Y are weights for the independent and dependent variables respectively, with w_X, $w_Y \geq 0$ and $w_X + w_Y = 1$. The weight factors must be a function of the estimated experimental error of the measured variable (er) compared to the standard deviation (SD) of the whole set of measurements of this variable. For a given pair of variables,

$$w_X = \left(\frac{er_X}{SD_X}\right) \Big/ \left(\frac{er_X}{SD_X} + \frac{er_Y}{SD_Y}\right) \quad (4)$$

In order to simplify the linear regression analyses, all possible cases were condensed to 2 categories or models: (I) $w_X = 0$, $w_Y = 1$; and (II) $w_X = w_Y = 0.5$ (Sokal & Rohlf 1995). Model I was used when X was temperature or salinity and Y was any biological or chemical variable. In these cases, $w_Y \gg w_X$, while model II was used when both X and Y were chemical or biological variables and $w_Y \approx w_X$. Differences between models I and II increase as the correlation coefficient (r) decreases.

RESULTS

Hydrographic scenarios and associated nutrient distributions

The characteristic wind features in the NW Iberian upwelling system can be seasonally identified from the time course of $<I_W>$ (Fig. 2a). The upwelling season was in September 1994 (surveys 9 and 10) and from March to September 1995 (surveys 22 to 34) and the downwelling season from November 1994 to February 1995 (surveys 13 to 20). Transient conditions from upwelling to downwelling, the autumn transition (October 1994, surveys 11 and 12), and from downwelling to upwelling, the spring transition (March 1995, surveys 21 and 22), were sampled too. The mean $<I_W>$ during the upwelling season was 353 m^3 s^{-1} km^{-1}, very close to the long-term average of 333 m^3 s^{-1} km^{-1} from 1966 to 1995 (Lavín et al. 1991, Nogueira et al. 1997a).

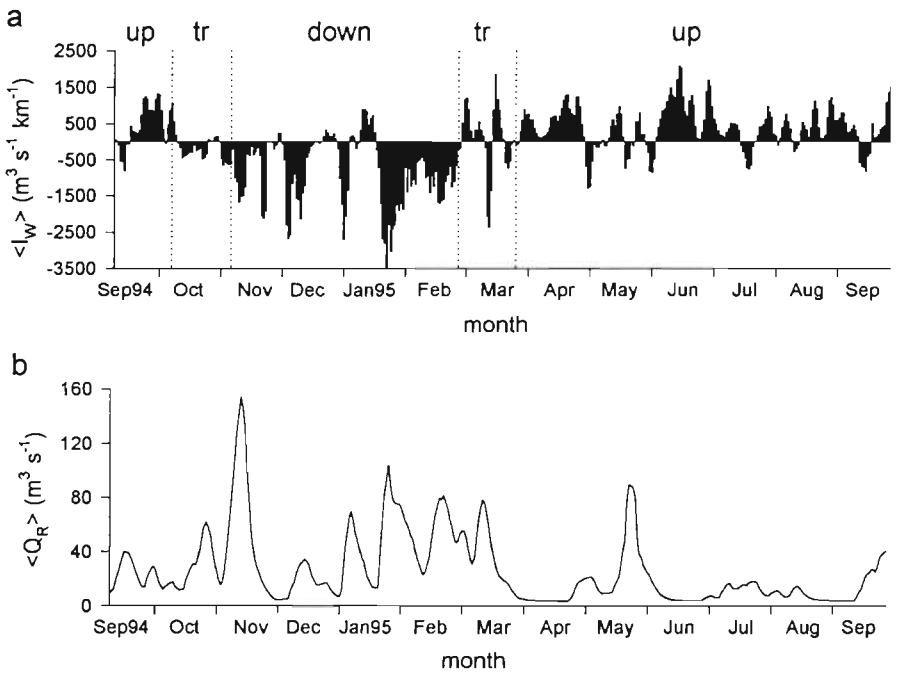

Fig. 2. Time course of (a) average upwelling index, $<I_w>$ (m^3 s^{-1} km^{-1}), calculated at 43°N, 11°W, and (b) average runoff, $<Q_R>$ (m^3 s^{-1}), from September 1994 to September 1995. $<Q_R>$ was estimated as the sum of a function of precipitation and the flow from the river Oitaben regulated by the Eiras reservoir to the Ría de Vigo. Wind features are indicated by 'up' (upwelling seasons), 'tr' (transitions) and 'down' (downwelling seasons)

The response of the water column to alternative upwelling and relaxation conditions during the upwelling season can be appreciated in the peaks and troughs of the 13°C isotherm (Fig. 3a), approximately the upper limit of ENACW (Fraga 1981, Fraga et al. 1982). Upwelling conditions were sampled during surveys 10, 22, 24, 27, 31, 32 and 34. The upwelling season was characterised by limited runoff (Fig. 2b), although high flows occurred in May 1995 (surveys 25 and 26), coinciding with fluctuating northerly-southerly winds, as during transient periods. $\overline{N}^2$ (Fig. 3c) decreased during upwelling conditions, and increased during upwelling relaxations (surveys 9, 23, 25, 26, 29 and 30). The pycnocline was located between 6 and 12 m (Fig 3a). Therefore, the sample at 15 m was usually in the lower layer.

During the downwelling season, the highest $<Q_R>$ were observed by October–November 1994 (surveys 12 to 14), although surface salinity at the time-series station was not the lowest. Lower surface salinity during February 1995 (surveys 18 and 19) showed that the convergence associated with the downwelling front moved to the shelf. Anomalous upwelling conditions were sampled during January (survey 17). High stability during the downwelling season ($\overline{N}^2 > 2$ min^{-2}) was maintained by strong continental runoff (Fig. 2b). The pycnocline was also observed between 6 and 12 m, except for surveys 15 (strong homogenisation) and 18 and 19 (high runoff) during which the pycnocline was deeper.

During the autumn transition lower $\overline{N}^2$ and a deeper pycnocline (>14 m) were observed, due to strong vertical mixing generated by the reversed estuarine circulation (Rosón et al. 1997). In contrast, higher $\overline{N}^2$ and a shallower pycnocline (~10 m) were sampled during the spring transition. The relatively high runoff (Fig. 2b) increased the stability of the water column. The rising solar insolation and the high discharge from the rías can mask the effect of upwelling during the spring transition (Blanton et al. 1984, McClain et al. 1986, Tenore et al. 1995).

The time courses of ΣCO_2 and DIN (Fig. 4a, b) in the lower layer were obviously tied to the variability of the thermohaline properties (Fig. 3a, b). The inflows and outflows of ENACW during the upwelling season can be observed in the vertical displacement of the DIN and ΣCO_2 isolines. In addition, mineralization processes and sediment-water exchange, more evident during relaxation and moderate downwelling conditions, increased DIN and ΣCO_2 in the lower layer. Nutrients were transported to the surface layer during strong upwelling conditions. Relative NH_4^+ maxima were sampled during upwelling relaxations (surveys 9, 25, 26, 29 and 30; Fig. 4c) due to rapid ammonification of sinking particulate organic matter (POM), and during downwelling conditions (survey 33) due to net release from the sediments (Álvarez-Salgado et al. 1996a). During the downwelling season, the highest DIN and lowest ΣCO_2 were sampled in January (surveys 18 and 19) due to the strong freshwater influence. During November 1994 (survey 14), NH_4^+ maxima were found in both layers, because of the composite effect of advection of waters regenerated in the inner-

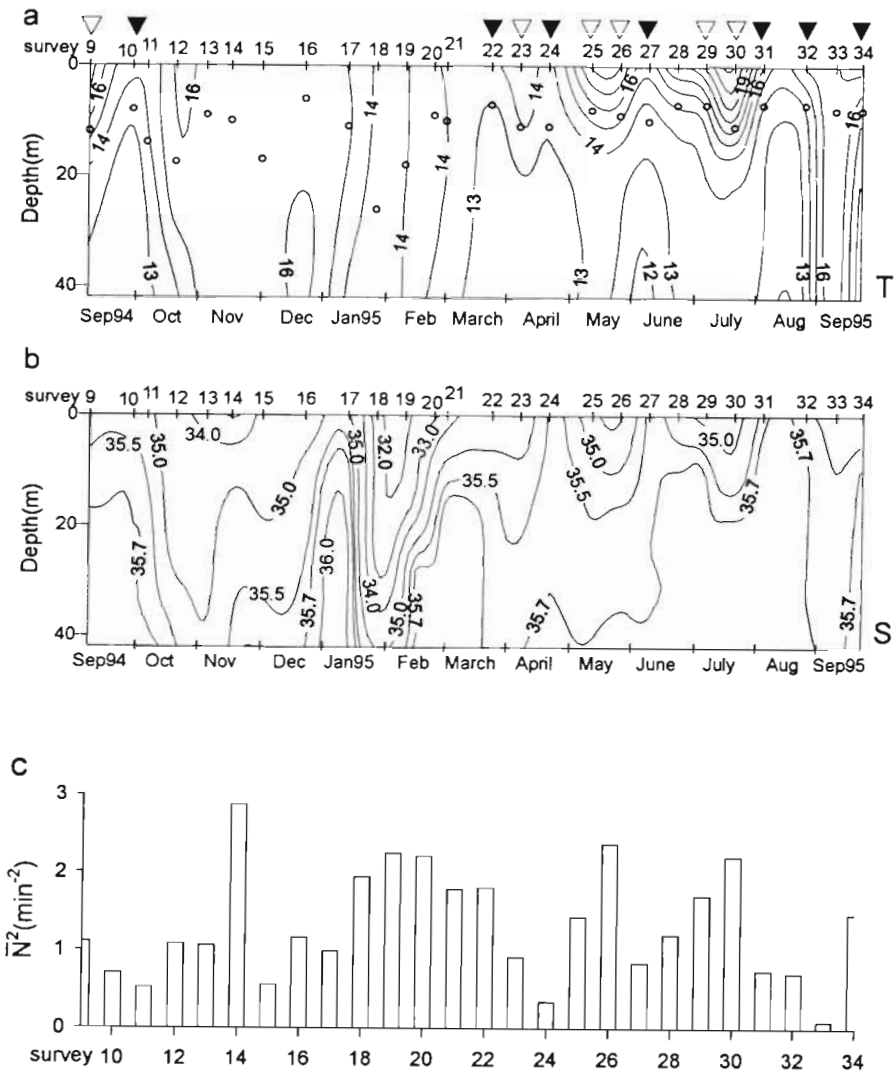

Fig. 3. Time course of (a) temperature (°C), (b) salinity, and (c) average stability $\bar{N}^2$ (min^{-2}) at the time-series station in the Ría de Vigo from September 1994 to September 1995. (o) Position of pycnocline; (▼) upwelling conditions and (▽) relaxation periods during the upwelling season

most part of the ría and ammonium released from the sediments (Pérez et al. 1992, Álvarez-Salgado et al. 1996b).

Chlorophyll *a* (chl *a*) maxima (Fig. 4d) appeared in the surface layer during the upwelling season (surveys 11, 22, 24, 25, 27, 29, 30, 31 and 34). Several maxima coincided with upwelling relaxations (surveys 11, 29 and 30), when growing phytoplankton accumulates in the upper layer just after an upwelling event because of reduced 'washout' compared to cells doubling time (Rosón et al. 1995, Álvarez-Salgado et al. 1996a). During the other relaxation periods high chl *a* was not sampled. This was likely because the surveyed days were at the end of prolonged periods of relaxation (>10 d), when nutrient replenishment was rather limited and the phytoplankton population succeeded to dinoflagellates (Figueiras & Rios 1993, Pazos et al. 1995). On the other hand, several chl *a* maxima occurred during upwelling conditions (surveys 22, 24, 31 and 34). These surveys coincided with the 'spin down' of upwelling pulses, after the lag time for adaptation of phytoplankton to the nutrient and light conditions of upwelling (Zimmerman et al. 1987). Finally, the chl *a* maximum observed during May 1995 (survey 27) developed under moderate upwelling conditions after a minor runoff event (Fig. 2b). Chl *a* was low in bottom waters except in surveys 23 and 28, due to sedimentation of the surface chl *a* maxima or strong bottom resuspension. During the downwelling season chl *a* was extremely low, as primary production was severely light limited (Fraga 1967, Nogueira et al. 1997a). However, an anomalous winter bloom (chl *a* >3 µg l^{-1}) was sampled in surface waters during December 1994 (survey 15).

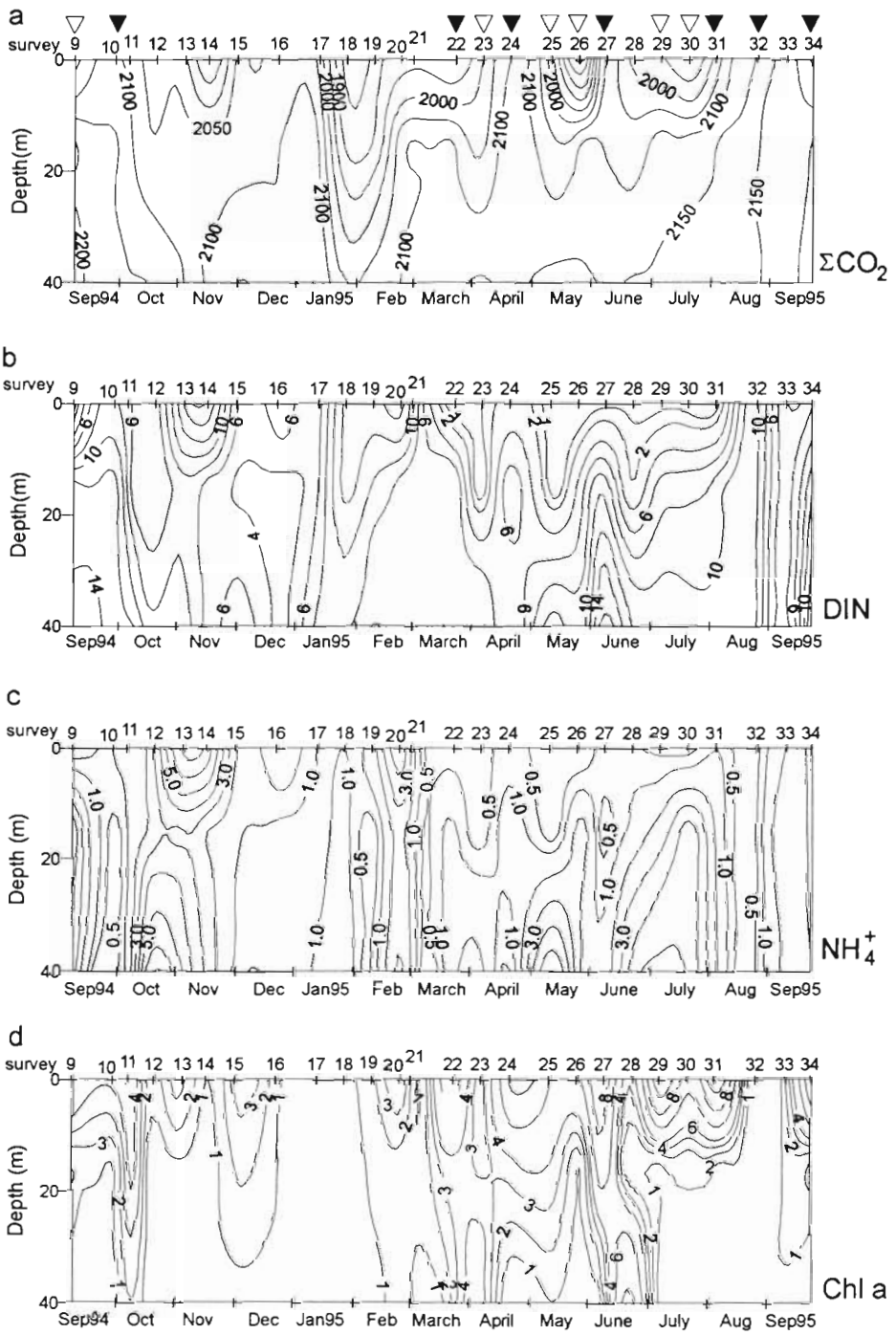

Fig. 4. Time course of (a) ΣCO_2 (µmol kg^{-1}), (b) DIN (µmol kg^{-1}), (c) ammonium (µmol kg^{-1}), and (d) chlorophyll *a* (µg l^{-1}) distributions at the time-series station in the Ría de Vigo from September 1994 to September 1995. (▼) Upwelling conditions and (▽) relaxation periods during the upwelling season

Particulate and dissolved organic matter distributions

The distributions of POC and PON (Fig. 5a, b) showed the expected decrease with depth. The average concentrations were 27.1 µM C and 4.0 µM N in the surface layer, 12.9 µM C and 1.8 µM N at 15 m and 16.9 µM C and 2.0 µM N at 40 m (Fig. 6a, b). Slightly higher average concentrations were recorded in the bottom than at 15 m. POM maxima were observed in the surface layer (surveys 12, 19, 20, 26, 27, 29, 30, 31 and 34), and in the bottom layer during surveys 22, 23 and 28. In general, POM maxima coincided with chl *a* maxima, as phytoplankton is the primary source of POM in the marine environment (Middelburg et al. 1993). However, chl *a* maxima sampled during the

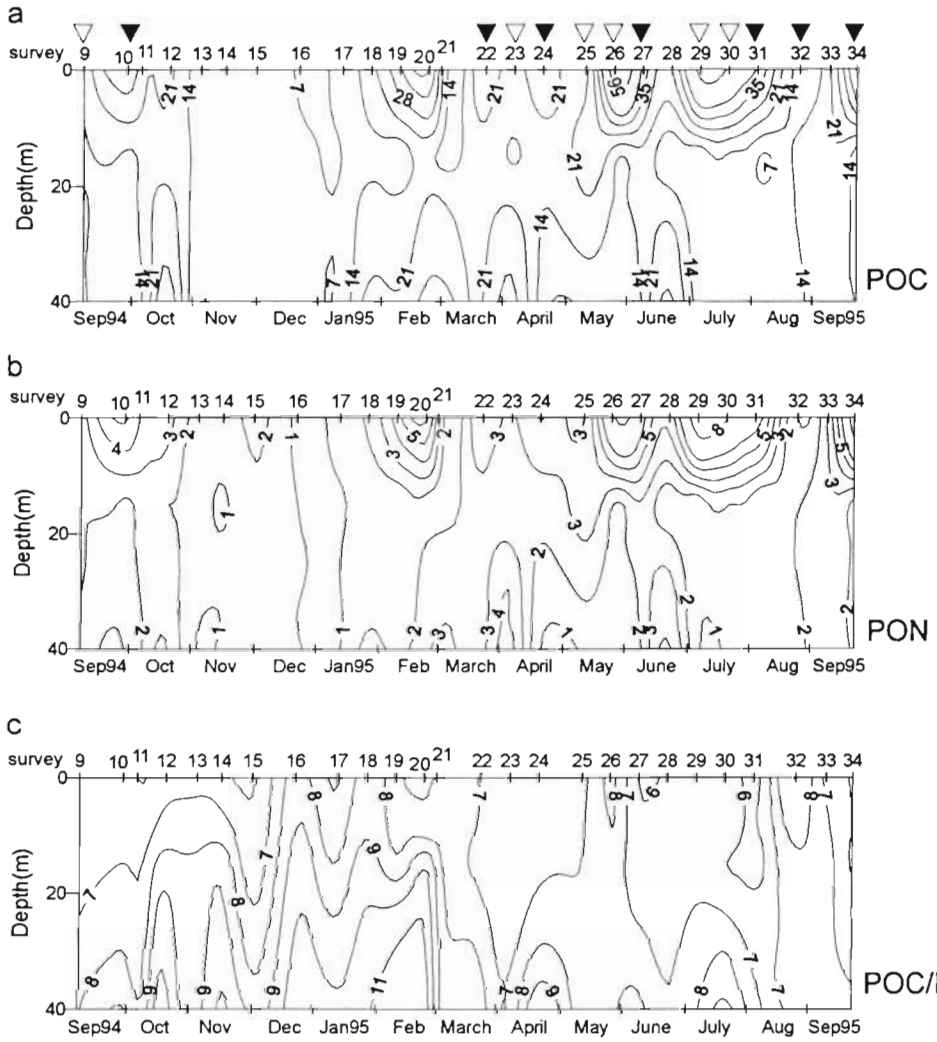

Fig. 5. Time course of (a) POC (μmol l^{-1}), (b) PON (μmol l^{-1}), and (c) POC/PON distributions at the time-series station in the Ría de Vigo from September 1994 to September 1995. (▼) Upwelling conditions and (▽) relaxation periods during the upwelling season

downwelling season (survey 15) and during March–April 1995 (surveys 22 and 24) did not indicate high POM values, and the POM maximum during survey 19 (high continental runoff) did not show high chl *a*. The rest of the downwelling season was characterised by low POM values. In spite of these differences, the direct correlation (model II) between PON and chl *a* yielded 0.70 (regression 1, Table 1). The correlation between POC and chl *a* was slightly lower ($r^2 \approx 0.60$; regression 2, Table 1). The average PON/chl *a* ratios were 1.3 (±0.8) mol N g^{-1} chl *a* in the surface layer, 1.6 (±1.2) mol N g^{-1} chl *a* at 15 m and 2.8 (±1.7) mol N g^{-1} chl *a* at 40 m.

The C/N molar ratio of POM (Fig. 5c) increased markedly with depth. The average C/N ratios were 6.9 in the surface layer, 7.4 at 15 m and 8.7 at 40 m (Fig 6c). The highest variability was observed at 40 m. Maximum values (>9) were recorded in the bottom layer during the downwelling season (surveys 16 to 20). POC and PON were obviously coupled, and the r^2 of the direct correlation (model II) was 0.92 (regression 3, Table 1). The origin intercept was not significantly different from zero.

All profiles showed a significant decrease of DOC and DON with depth (Fig. 7a, b). The average concentrations were 100 μM C and 6.8 μM N in surface waters, 83 μM C and 5.6 μM N at 15 m and 76 μM C and 5.0 μM N in bottom waters (Fig. 6d, e). Several high values of surface DOC caused a wide range of variation. Extreme concentrations were recorded during the upwelling season: the highest values (>100 μM C and >7 μM N) in the surface layer in upwelling relaxation conditions (surveys 9, 25, 26, 29 and 30) and the lowest values (<70 μM C and <4 μM N) in bottom upwelled waters. During the upwelling season, the vertical displacements of isolines from 60 to 75 μM C

and from 5 to 6 µM N traced the succession of upwelling and relaxation conditions.

During the downwelling season, the reversal in circulation provoked DOM homogenization and a subsurface maximum of 110 µM C and 8.5 µM N at 15 m during November 1994 (survey 13), coinciding with a relative chl *a* maximum. The rest of the downwelling season showed lower values of DOM with relative maxima during surveys 15 and 16 (coinciding with the winter bloom) and surveys 18 and 19 (coinciding with the surface salinity minimum).

The distribution of DOM (Fig. 7a, b) resembles that of temperature (T) (Fig. 3a), the latter being used as a marker of hydrographic changes. In fact, r^2 of the direct correlation between DOC and T (model I) for all samples was 0.46 (regression 4, Table 1). The origin intercept was not significantly different from zero. The correlation between DON and T was slightly lower (r^2 = 0.43; regression 5, Table 1). Phytoplankton production is also the ultimate source of DOM in the sea (Kirchman et al. 1991). However, the direct correlation between DOC and chl *a* (model II) yielded only r^2 = 0.26. Therefore, DOC and chl *a* distributions were not coupled over a short time scale. As the distribution of DOC was influenced by both physical and biological variables, the total correlation of DOC with T (model I) and chl *a* (model II) was considered too (r^2 = 0.53; regression 6, Table 1).

The distribution of the C/N molar ratio of DOM (Fig. 7c) did not change significantly with depth. The range of variation was 12 to 20, with an average value of ~15 for the whole data set (Fig. 6f). The time courses of DOC and DON distributions were similar: r^2 of the direct regression between DOC and DON (model II) was 0.57 (regression 7, Table 1). The correlation obtained between both variables and the substantial difference between the direct DOC/DON ratio (~15) and the slope of the regression line (~12) are noteworthy. The origin intercept (17 µM) is the

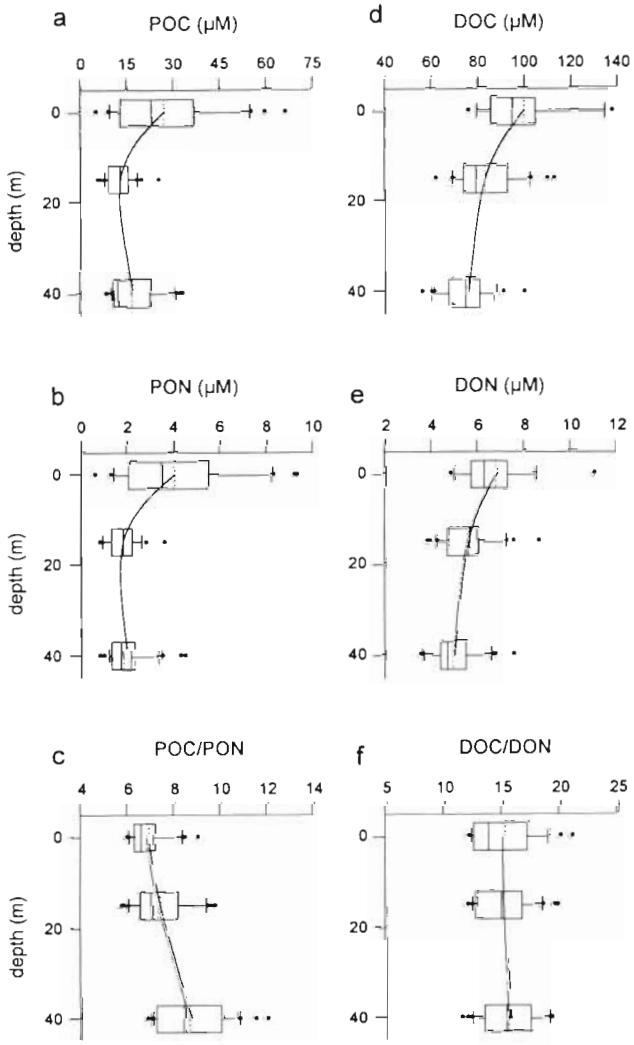

Fig. 6. Box and whisker plot of (a) POC, (b) PON, (c) POC/PON, (d) DOC, (e) DON, and (f) DOC/DON at the surface, 15 m and 40 m depth. Fifty percent of the data are included within the limit of the boxes and the caps represents the 10th and 90th percentiles. (—) Median; (···) mean. The mean profile is also shown

Table 1. Selected linear regressions among the different variables related to organic matter pools: particulate organic nitrogen (PON), particulate organic carbon (POC), dissolved organic carbon (DOC), dissolved organic nitrogen (DON), chlorophyll *a* (chl *a*) and temperature (T). n = 76, $p < 0.001$. Numbers in brackets are the standard error of the dependent variable estimate and the standard errors of the coefficients

No.	Variables	Equation	r^2
1	PON vs chl *a*	PON (±1.1) = 0.9(±0.2) + 0.68(±0.05)chl *a*	0.70
2	POC vs chl *a*	POC (±7.3) = 8.4(±1.3) + 3.1(±0.3)chl *a*	0.59
3	POC vs PON	POC (±3.5) = 7.2(±0.1)PON	0.92
4	DOC vs T	DOC (±13) = 5.9(±0.1)T	0.46
5	DON vs T	DON (±1.1) = 0.39(±0.01)T	0.43
6	DOC vs T, chl *a*	DOC (±12) = −7.5(±0.8) + 5.6(±0.2)T + 4.9(±0.5)chl *a*	0.53
7	DOC vs DON	DOC (±12) = 17(±10) + 12(±1)DON	0.57
8	DOC vs T, DON	DOC (±11) = −30(±13) + 3.3(±0.4)T + 12(±1)DON	0.62

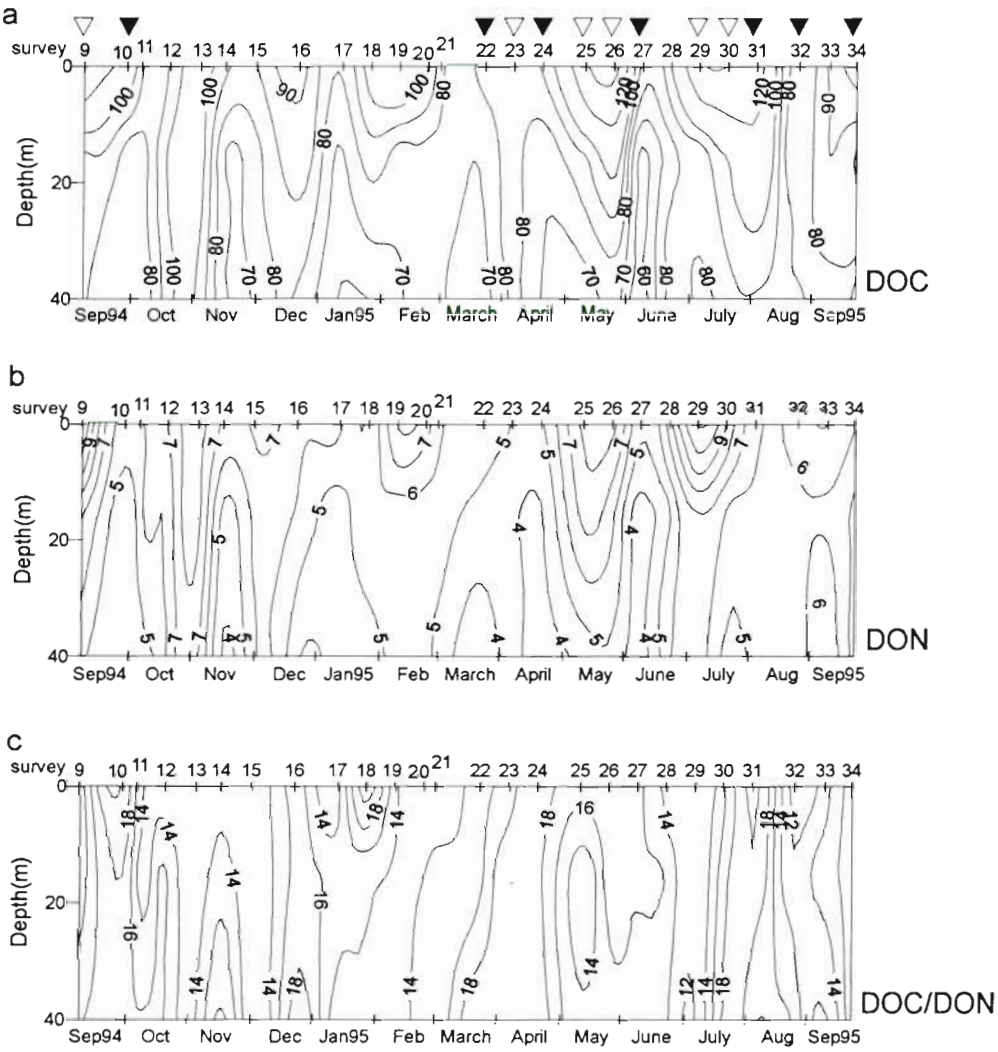

Fig. 7. Time course of (a) DOC (μmol l^{-1}), (b) DON (μmol l^{-1}), and (c) DOC/DON distributions at the time-series station in the Ría de Vigo from September 1994 to September 1995. (▼) Upwelling conditions and (▽) relaxation periods during the upwelling season

DOC not associated with DON, i.e. carbonaceous material.

In order to examine independently the effect of temperature and DON in the DOC distribution, the correlation of DOC with T (model I) and DON (model II) was considered. r^2 for this correlation was 0.62 (regression 8, Table 1). Consequently, up to 62% of the variability observed in the DOC distribution can be explained by a linear combination of the T and DON distributions. It also showed that the origin intercept was temperature dependent (it increased with increasing temperature). In addition, the coefficient for DON, independent of the variation of temperature, was kept at 12. It is remarkable that if model I had been considered for both T and DON, the coefficient for DON would have been as low as 6.5, leading to a quite different discussion. Therefore, the correct choice of the regression model is crucial.

Estimation of surface 'DOM excess'

A DOM excess was observed in surface waters as compared to bottom waters at the time-series station (Fig. 7a, b) throughout the study period. A rough estimation of this excess could be performed with a simple 2-endmember mixing model, one endmember being the freshwater input (F), and the other endmember the bottom water at the time-series station (B). For DOC we can write:

$$DOC_{EXC} = DOC_S - \left(\frac{S_S}{S_B} \cdot DOC_B + \frac{S_B - S_S}{S_B} \cdot DOC_F \right) \quad (5)$$

where DOC_{EXC} is DOC excess, DOC_S and S_S are DOC and salinity at the surface, DOC_B and S_B are DOC and salinity at the bottom, and DOC_F is DOC in the freshwater discharge (see Fig. 8a). The same equation can be written for DON. The freshwater contribution to the

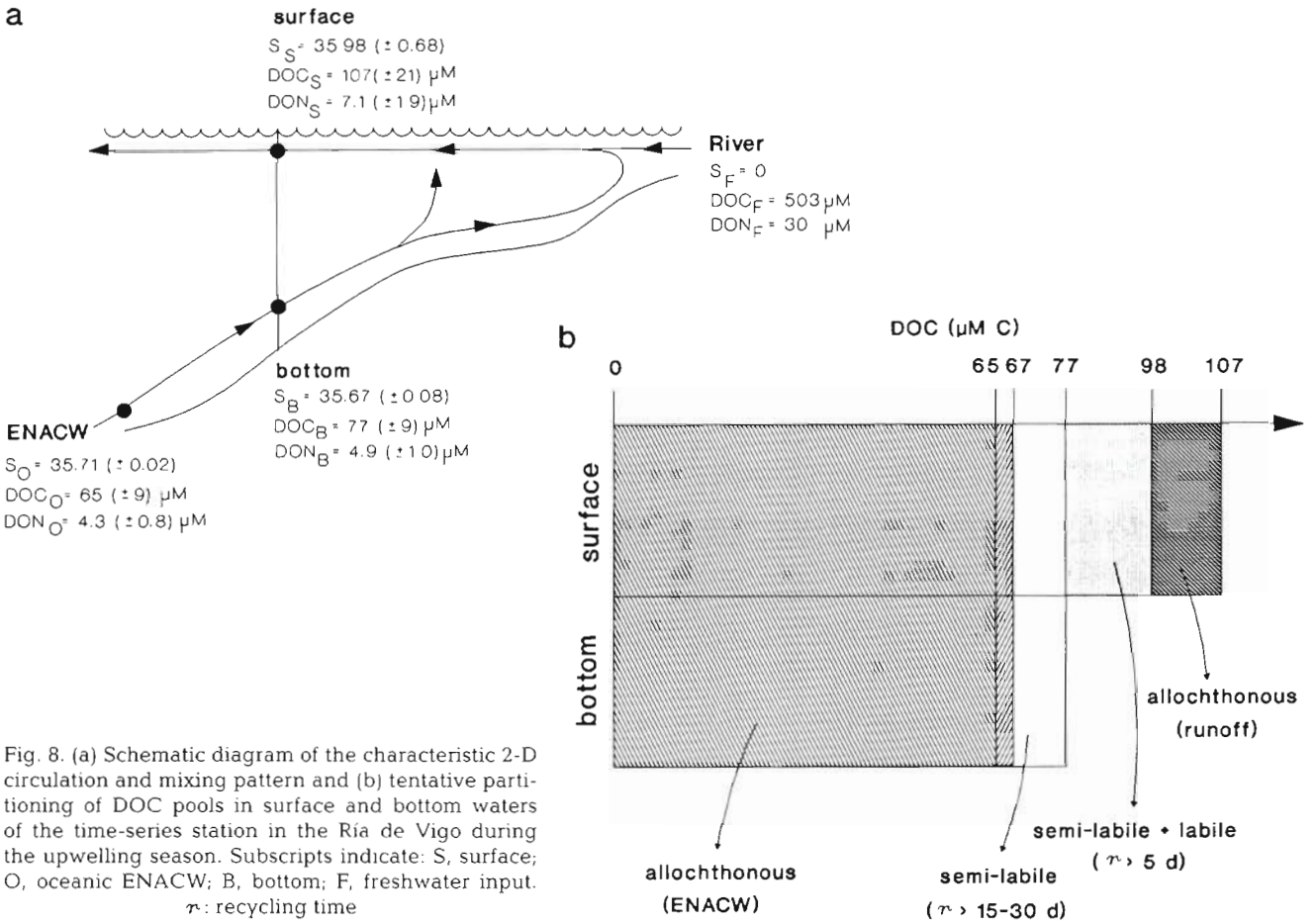

Fig. 8. (a) Schematic diagram of the characteristic 2-D circulation and mixing pattern and (b) tentative partitioning of DOC pools in surface and bottom waters of the time-series station in the Ría de Vigo during the upwelling season. Subscripts indicate: S, surface; O, oceanic ENACW; B, bottom; F, freshwater input. τ: recycling time

time-series station was the sum of continental runoff (R) and waste water (W). So, DOC_F can be estimated as:

$$DOC_F = \frac{DOC_R \cdot Q_R + DOC_W \ Q_W}{Q_R + Q_W} \quad (6)$$

The average runoff (Q_R) was 44.7 $m^3 s^{-1}$ for the downwelling season and 15 $m^3 s^{-1}$ for the upwelling season (Fig. 2a). The waste water flow (Q_W) was ~0.5 $m^3 s^{-1}$ (Prego et al. 1990). The evaporation-precipitation budget has been neglected in our discussion. Annual average DOC and DON concentrations on R and W were 400 µM C, 20 µM N and 3600 µM C, 325 µM N respectively. DOC_R and DON_R were estimated from samples taken in the innermost part of the ría, and extrapolated to zero salinity. DOC_W and DON_W were calculated from samples taken near the domestic waste poured into the commercial port of Vigo (Doval & Pérez 1997). Average DOC_F and DON_F were 435 µM C and 23 µM N for the downwelling season and 503 µM C and 30 µM N for the upwelling season.

To calculate the DOM excess we need to assume that steady-state conditions occurred during the flushing time from the river mouth up to the time-series station, ~5 d (Ríos 1992). The average excess for the upwelling season was 21 µM C and 1.7 µM N, the freshwater contribution to the time-series station being 9 µM C and 0.6 µM N. In contrast, for the downwelling season the DOC and DON excess in surface waters was slightly negative: −6 µM C and −0.1 µM N. The freshwater contribution, as high as 25 µM C and 2.1 µM N, was responsible for the higher DOM levels in the surface layer as compared to the bottom layer during the downwelling season. Consequently, during the upwelling season a net export of DOM (the DOM excess) occurred via surface waters with an average C/N molar ratio of ~12 (= 21/1.7).

Estimation of DOM pools during the upwelling season

The labile and semi-labile pools are the most interesting fractions of DOM due to the biogeochemical properties associated with them. DOM partitioning has been made in oligotrophic gyres by several authors using a simple 1-dimensional model (Copin-Montégut & Avril 1993, Carlson & Ducklow 1995, Cherrier et al.

1996). However, the influence of horizontal advection on DOM distributions at the time-series station of the Ría de Vigo must be considered. Therefore, a 2-end-member mixing model was used to characterise the DOM pool during the upwelling season, when net production occurred.

The DOC in bottom waters of the time-series station expected from mixing of oceanic ENACW and surface water of this station (DOC'_B) can be estimated as:

$$DOC'_B = \left(\frac{S_O - S_B}{S_O - S_S}\right) \cdot DOC_S + \left(\frac{S_B - S_S}{S_O - S_S}\right) \cdot DOC_O \quad (7)$$

where S_O and DOC_O are salinity and DOC in upwelled oceanic ENACW. The ENACW sampled during the same period on shelf bottom waters off the Ría de Vigo (42° 7.8' N, 9° 7.5' W, 140 m depth; O.S. in Fig. 1) was advected to the time-series station by the upwelling-enhanced residual circulation. The average S_O, DOC_O and DON_O during the upwelling season are shown in Fig. 8a. Such upwelled DOM was clearly allochthonous to the ría, and must be essentially refractory.

We observed that the average DOC in the lower layer of the time-series station (DOC_B; Fig. 8a) was higher than the calculated DOC'_B (67 µM C). The difference, ~10 µM C (Fig. 8b), was the net increase of DOC due to net production in bottom waters within the time necessary to cover the 31 km distance between the shelf station and the time-series station (Fig. 1). Assuming an average velocity in the range of 1 to 2 km d^{-1}, the produced DOC must have a recycling time >15 to 30 d. This is semi-labile DOC. The difference between DOC_O and DOC'_B is the increase of DOC due to mixing of ENACW with the overlying water by turbulent vertical mixing (~2 µM C). Finally, the total DOC excess in surface waters as compared to bottom waters of the time-series station, ~30 µM C (Fig. 8b), was due to the freshwater contribution (~9 µM C) and the DOC produced in the inner ría (~21 µM C) during the flushing time (~5 d; see previous section).

With respect to DON, the calculated DON'_B was 4.5 µM N and the semi-labile DON produced in the bottom layer between the 2 reference stations was 0.4 µM N. The increase of DON due to mixing was 0.2 µM N. Finally, the total DON excess in surface waters of the time-series station (~2.2 µM N) arises from the freshwater contributions (~0.5 µM N) and DON produced in the inner ría (~1.7 µM N). The C/N ratio of DOM was much higher in the allochthonous ENACW (~15) than in the more labile fraction (~12), as expected.

DISCUSSION

The higher average values of POC and PON at 40 m than at 15 m could be due to the sedimentation of surface blooms, resuspension of organic-rich sediment (driven by the effects of upwelling and tides, ~3 m) or zooplankton accumulation (Fraga & Vives 1961, Fraga 1967). The observed increase of the C/N ratio of POM towards the bottom (from 6.7 to 8) was due to the more intense recycling of nitrogenous as compared to carbonaceous compounds and the resuspension of C-rich POM (Copin-Montégut & Copin-Montégut 1983). Relatively high bottom DOM concentrations were measured too at the time-series station during October–November 1994 and between July and September 1995. Bottom resuspension of DOM associated with nutrient fluxes from the sediments and partial degradation of settled POM could be the reasons behind the net production of DOM in the bottom layer as compared to upwelled ENACW (Prego 1993a, Álvarez-Salgado et al. 1996a). Following regression 1 (Table 1), autotrophs represented about 65% of the total PON in the whole water column. This percentage was estimated from the relative contribution of the slope multiplied by the average chl *a* compared to the average PON concentration. The direct PON/chl *a* ratio showed a marked increase between 15 and 40 m (from 1.6 to 2.8 mol N g^{-1} chl *a*), indicating a higher contribution of heterotrophs and, especially, detritus at 40 m.

Following the description of the time course of organic matter pools, nutrient-rich and DOM-poor subsurface waters are transported to the surface layer during the 'spin up' phase of upwelling events. Phytoplankton growth and accumulation occurs at the expense of the upwelled nutrients during the 'spin down' phase, as indicated by chl *a* and POM. Finally, DOM accumulation in the surface layer takes place at the end of the bloom, after several days of non-wind-forced conditions. This sequence of events takes place periodically during the upwelling season in response to the wind regime. Hydrographic control of phytoplankton growth and accumulation is a common phenomenon in coastal upwelling systems at temperate latitudes (Barber & Smith 1981, Zimmerman et al. 1987, Álvarez-Salgado et al. 1996b). DOC accumulation at the end of blooms seems to be a quite general pattern too (Kirchman et al. 1991, 1994, Norrman et al. 1995, Chen et al. 1996). Although Carlson & Ducklow (1995) found that physical control has an important influence on the DOC distribution in the equatorial upwelling of the Central Pacific, the lack of DOM data in coastal upwelling areas does not allow one to generalise this expectable behaviour. This behaviour is also observed in DON accumulation during the upwelling season, which is an interesting issue as nitrogen is usually the limiting element of primary production in upwelling areas. Surface DON excess in these systems (mainly after prolonged relaxations, when surface nutrients are depleted) implies the presence of DON

not immediately available (recycling time >5 d) to the microbial loop organisms. However, the C/N ratio of the DOM excess, about twice the Redfield ratio, pointed to a higher accumulation of DOC rather than DON or to a more efficient utilisation of produced DON in nitrogen limited systems.

The high C/N ratio of DOM (Jackson & Williams 1985, Hansell et al. 1993, Sambrotto et al. 1993, Williams 1995, Chen et al. 1996) is usually related to a carbohydrate excess (Ittekkot et al. 1981, Benner et al. 1992). The wide range of C/N values is due to the variable molecular composition of DOM (Jackson & Williams 1985), which explains the lower correlation between DOC and DON compared to the correlation between POC and PON. The origin intercept, i.e. the fraction of DOC that does not covary with nitrogen, increased with temperature (regression 8, Table 1). Considering the average temperature for bottom and surface waters, the origin intercept ranged from 15 to 23 µM C. This was 20 and 23% of the total DOC in bottom and surface waters respectively. [The origin intercept is responsible for the large difference between the DOC:DON molar ratios (15) observed from the averaging of the data and from the regression slope (12; regression 7, Table 1).] These fractions were similar to the percentage of total carbohydrate as compared to DOC reported by Pakulski & Benner (1994) in surface ocean waters (21 ± 7%).

The DOM freshwater contribution to the time-series station was relevant for the whole period studied. The average contribution represented ~30% of the total surface DOC excess (30 µM C) during the upwelling season. During the downwelling season, the freshwater contribution exceeded the DOM excess in surface waters. Several authors have suggested that riverine inputs are a source of DOC accumulation in coastal waters (Aminot et al. 1990, Zweifel et al. 1995). The estimated riverine DOC (~400 µM C) was similar to the average concentration in European rivers, ~350 to 420 µM C (Meybeck 1982, Ludwig et al. 1996). The relative DOM contribution from waste water as compared to the total freshwater contribution was 23 and 35% for DOC and DON respectively during the upwelling season and 9 and 15% during the downwelling season.

With respect to the lability of DOM, considering the allochthonous freshwater and ENACW contributions as refractory, the inert pool was 72 µM C and 4.8 µM N during the upwelling season. Therefore, it made up about 70% of the DOC and DON levels in surface waters. These amounts are similar to the percentage of refractory DOC reported in different areas worldwide (Copin-Montégut & Avril 1993, Carlson & Ducklow 1995, Thomas et al. 1995, Chen et al. 1996). However, part of the allochthonous DOC carried by ENACW was semi-refractory. DOC of oceanic ENACW at 300 to 400 m was ~60 µM C, and DOC decreased to ~50 µM C in deeper waters of the Eastern North Atlantic (X. A. Álvarez-Salgado & A. E. J. Miller unpubl.). So, considering that the properly refractory oceanic pool is only 50 µM C, the estimated percentage of refractory DOC in the Ría de Vigo should be lowered to ~60% In addition, part of the refractory DOC in ENACW upwelled to the surface could be photochemically degraded by the ultraviolet radiation (UVR) into biologically labile compounds (Kieber et al. 1990, Mopper et al. 1991, Wetzel et al. 1995). On the other hand, semi-refractory properties of the riverine DOM have been recently proposed too (Carlsson & Graneli 1993, Carlsson et al. 1995, Zweifel et al. 1995). Moreover, refractory riverine DOM could be photochemically degraded into biologically available compounds (Bushaw et al. 1996). Photochemical degradation of DON to NH_4^+ (Bushaw et al. 1996) could be especially important in nitrogen limited areas. We do not know the photochemically degradable fractions. For these reasons, further studies are necessary, particularly in areas where upwelling of subsurface water is favoured.

Labile DOC turnover was estimated to be between 2 and 11 d (Kirchman et al. 1991, Norrman et al. 1995, Cherrier et al. 1996). As we have estimated that the DOM excess in surface waters during the upwelling season was produced in ~5 d; this excess can be considered a mixture of labile and semilabile material. In fact, the C/N molar ratio of the DOM excess (~12), which coincides with the slope of the direct regression between DOC and DON (regression 7, Table 1), was much lower than the direct C/N molar ratio of DOM (~15). Bacterial production and respiration yields must be performed to properly quantity the lability of the DOM excess (Norrman et al. 1995, Cherrier et al. 1996, Giorgio et al. 1997).

The average net primary production in surface waters at the time-series station during the upwelling season was estimated by Moncoiffé (1995) as 25.2 µM O_2 d^{-1}, using the O_2 incubation method. If the stoichiometric ratio R_C = 1.4, characteristic of a system in which nitrate supports net primary production (Fraga & Pérez 1990, Laws 1991, Anderson 1995) is used, then the average net production will be 18 µM C d^{-1} The net DOC excess in surface waters (21 µM C) was produced in the inner ría within ~5 d. Therefore, the net average DOC production, 4.2 µM C d^{-1}, was ~23% of net carbon production in surface waters of the time-series station. This percentage was in the range of DOC excretion for phytoplankton, 0 to 30%, measured by other researchers (Norrman et al. 1995). For nitrogen, based on the C/N ratio of surface POM (6.9), the average net production would be 2.61 µM N

d^{-1} (= 18/6.9) The average DON production was 0.34 µM N d^{-1} (= 1.7/5), i.e. ~13% of net nitrogen production in surface waters.

About 80% of the TOC and 70% of the TON was DOC and DON for the whole water column. If only the DOM_{EXC} were considered, the numbers would be as low as ~40% for carbon and 30% for nitrogen. These values indicate that POM was the most important fraction of net total organic matter produced in the inner ría. This is because the Ría de Vigo is a highly productive ecosystems in which production of POM is largely favoured. Higher contributions of DOC_{EXC} to TOC were estimated in oligotrophic areas (Copin-Montégut & Avril 1993, Carlson & Ducklow 1995, Cherrier et al. 1996).

CONCLUSIONS

DOM in the central part of the Ría de Vigo was strongly influenced by physical and biological processes. Observed DOM levels are partially due to the external inputs to the embayment: (1) oceanic ENACW; (2) continental runoff; and (3) waste water. In addition, net accumulation of DOM in surface waters has been observed during the upwelling season, while the system was close to balance during the downwelling season. Phytoplankton growth and accumulation occurs following nutrient transport to the surface during the 'spin up' phase of an upwelling pulse. Biomass decays and DOM accumulates during the subsequent upwelling relaxation. From the point of view of nutrients and chlorophyll *a* changes, the Ría de Vigo paralleled other coastal upwelling systems in temperate waters. Observed DOM changes could be a general pattern for upwelling systems.

The DOM excess was a mixture of labile and semilabile material which recycled in >5 d. DOC and DON excess represented ~23 and ~13% of net primary production, respectively. The average $DOC_{EXC}/(DOC_{EXC}$ + POC) ratio in surface waters was ~0.40. For nitrogen it was ~0.30. These fractions indicated that net POM production exceeded DOM production in the inner ría. In contrast, DOC and DON were about 77 and 60%, respectively, of organic matter in surface waters during the upwelling season. Therefore, the partitioning of DOM is essential to correctly estimate DOM export from surface waters.

In the case of nitrogen, the limiting nutrient in these embayments, the DON excess in surface waters during the upwelling season indicates the accumulation of a fraction of DON not immediately available to microbial loop organisms. However, the C/N ratio of DOM excess (~12) showed a relatively higher accumulation of C-rich biomolecules.

Acknowledgements. The authors thank the members of the group of oceanography from the Instituto de Investigacións Mariñas and the Instituto Español de Oceanografía who participated in the surveys and the crew of the RV 'Jose Mª Navaz' for their valuable help. We also thank R. Penín and M. V. González for the analysis of particulate organic matter and chlorophyll *a*; T. Rellán for the determination of carbon system variables; and M. J. Pazó for nutrient measurements. A fellowship from the EC MAS2 project CT93-0065 allowed M.D.D. to carry out this work. X.A.A.S. was funded by a 'contrato de Incorporación' of the Spanish 'Ministerio de Educación y Ciencia'. This study was partly financed by the 'Comisión Interministerial de Ciencia y Tecnología (CICYT)' grant No. AMB92-0165.

LITERATURE CITED

Álvarez-Salgado XA, Castro CG, Pérez FF, Fraga F (1997) Nutrient mineralization patterns in shelf waters of the western Iberian upwelling. Cont Shelf Res 17: 1247–1270

Álvarez-Salgado XA, Pérez FF, Fraga F (1992) Determination of nutrient salts by automatic methods both in seawater and brackish water: the phosphate blank. Mar Chem 39: 311–319

Álvarez-Salgado XA, Rosón G, Pérez FF, Figueiras FG, Pazos Y (1996a) Nitrogen cycling in an estuarine upwelling system, the Ría de Arousa (NW Spain). I. Short-time-scale patterns of hydrodynamic and biogeochemical circulation. Mar Ecol Prog Ser 135:259–273

Álvarez-Salgado XA, Rosón G, Pérez FF, Figueiras FG, Ríos AF (1996b) Nitrogen cycling in an estuarine upwelling system, the Ría de Arousa (NW Spain). II. Spatial differences in the short-time-scale evolution of fluxes and net budgets. Mar Ecol Prog Ser 135:275–288

Álvarez-Salgado XA, Rosón G, Pérez FF, Pazos Y (1993) Hydrographic variability off the Rías Baixas (NW Spain) during the upwelling season. J Geophys Res 98: 14447–14455

Aminot A, El-Sayed MA, Kerouel R (1990) Fate of natural and anthropogenic dissolved organic carbon in the macrotidal Elorn estuary (France). Mar Chem 29:255–275

Anderson LA (1995) On the hydrogen and oxygen content of marine phytoplankton. Deep Sea Res I 42:1675–1680

Azam F, Fenchel T, Field JG, Gray JS, Meyer-Reil LA, Thingstad F (1983) The ecological role of water column microbes in the sea. Mar Ecol Prog Ser 10:257–273

Bakun A (1973) Coastal upwelling indices, west coast of North America, 1946–71, NOAA Tech Rep NMFSSSRF-671

Barber RT, Smith RL (1981) Coastal upwelling ecosystems. In: Longhurst AR (ed) Analysis of marine systems. Academic Press, San Diego, p 31–68

Benner R, Pakulski JD, McCarthy M, Hedges JI, Hatcher PG (1992) Bulk chemical characteristic of dissolved organic matter in the ocean. Science 255:1561–1564

Blanton JO, Tenore KR, Castillejo F, Schwing FB, Atkinson LP, Lavin A (1987) The relationship of upwelling to mussel production in the rías on the western coast of Spain. J Mar Res 45:497–511

Bronk DA, Glibert PM, Ward BB (1994) Nitrogen uptake, dissolved organic nitrogen release, and new production. Science 265:1843–1846

Bushaw KL, and 8 co-authors (1996) Photochemical release of available nitrogen from aquatic dissolved organic matter. Nature 381:404–407

Carlson CA, Ducklow HW (1995) Dissolved organic carbon in the upper ocean of the central equatorial Pacific Ocean, 1992; daily and finescale vertical variations. Deep Sea Res II 42:639–656

Carlson CA, Ducklow HW, Michaels AF (1994) Annual flux of dissolved organic carbon from the euphotic zone in the North-western Sargasso Sea. Nature 371:405–408

Carlsson P, Granéli E (1993) Availability of humic bound nitrogen for coastal phytoplankton. Estuar Coast Shelf Sci 36:433–447

Carlsson P, Granéli E, Tester P, Boni L (1995) Influences of riverine humic substances on bacteria, protozoa, phytoplankton, and copepods in a coastal plankton community. Mar Ecol Prog Ser 127:213–221

Copin-Montégut G, Avril B (1993) Vertical distribution and temporal variation of dissolved organic carbon in the North Western Mediterranean Sea. Deep Sea Res I 40: 1963–1972

Copin-Montégut C, Copin-Montégut G (1983) Stoichiometry of carbon, nitrogen, and phosphorus in marine particulate matter. Deep Sea Res I 30:31–46

Chen RF, Fry B, Hopkinson CS, Repeta DJ, Peltzer ET (1996) Dissolved organic carbon on Georges Bank. Cont Shelf Res 16:409–420

Chen W, Wangersky PJ (1996) Rates of microbial degradation of dissolved organic carbon from phytoplankton cultures. J Plankton Res 18:1521–1533

Cherrier J, Bauer JE, Druffel ERM (1996) Utilization and turnover of labile dissolved organic matter by bacterial heterotrophs in eastern North Pacific surface waters. Mar Ecol Prog Ser 139:267–279

Doval MD, Fraga F, Pérez FF (1997a) Determination of dissolved organic nitrogen in seawater using Kjeldahl digestion after inorganic nitrogen removal. Oceanol Acta 20:(in press)

Doval MD, Nogueira E, Pérez FF (1997b) Spatio-temporal variability of the thermohaline and biogeochemical properties and dissolved organic carbon in a coastal embayment affected by upwelling: the Ría de Vigo. J Mar Syst (in press)

Doval MD, Pérez FF (1997) Determinación de carbono orgánico disuelto en la Ría de Vigo. VIII Seminario Ibérico de Química Marina (in press)

Figueiras FG, Jones KJ, Mosquera AM, Álvarez-Salgado XA, McDougall N (1994) Red tide assemblage formation in an estuarine upwelling ecosystem: Ría de Vigo. J Plankton Res 16:857–878

Figueiras FG, Niell FX (1987) Relaciones entre carbono, nitrógeno y clorofila a en la ría de Pontevedra, NO de España. Invest Pesq 51:3–21

Figueiras FG, Ríos AF (1993) Phytoplankton succession, red tides and hydrographic regime in the Rías Bajas of Galicia. In: Smayda TJ, Shimizu Y (eds) Toxic marine phytoplankton. Elsevier, New York, p 239–244

Fraga F (1960) Variación estacional de la materia organica suspendida y disuelta en la Ría de Vigo. Influencia de la luz y la temperatura. Invest Pesq 17:127–140

Fraga F (1967) Hidrografía de la Ría de Vigo 1962, con especial referencia a los compuestos de nitrógeno. Invest Pesq 31:145–259

Fraga F (1976) Fotosíntesis en la Ría de Vigo. Invest Pesq 40: 151–167

Fraga F (1981) Upwelling off the Galician coast, northwest Spain. In: Richards FA (ed) Coastal upwelling. Coastal and estuarine science 1, Washington, DC, p 176–182

Fraga F, Mouriño C, Manríquez M (1982) Las masas de agua en la costa de Galicia: junio–octubre. Result Exped Cient 10:51–77

Fraga F, Pérez FF (1990) Transformaciones entre composición química de fitoplancton, composición elemental y relación de Redfield. Scientia Mar 54:69–76

Fraga F, Vives F (1961) La descomposición de la materia orgánica nitrogenada en el mar. Invest Pesq 19:65–79

Giorgio PA, Cole JJ, Cimbleris A (1997) Respiration rates in bacteria exceed phytoplankton production in unproductive aquatic systems. Nature 385:148–151

Hansell DA (1993) Results and observations from the measurement of DOC and DON in seawater using a high-temperature catalytic oxidation technique. Mar Chem 41: 195–202

Hansen HP, Grasshoff K (1983) Automated chemical analysis. In: Grasshoff K, Ehrhardt M, Kremling K (eds) Methods of seawater analysis. Verlag Chemie, Weinheim, p 347–395

Ittekkot V, Brockmann U, Michaelis W, Degens ET (1981) Dissolved free and combined carbohydrates during a phytoplankton bloom in the northern North Sea. Mar Ecol Prog Ser 4:299–305

Jackson GA, Williams PM (1985) Importance of dissolved organic nitrogen and phosphorus to biological nutrient cycling. Deep Sea Res 32:223–235

Jumars PA, Penry DL, Baross JA, Perry MJ, Frost BW (1989) Closing the microbial loop: dissolved organic carbon pathway to heterotrophic bacteria from incomplete ingestion, digestion and adsorption in animals. Deep Sea Res 36: 483–495

Kieber RJ, Zhou X, Mopper K (1990) Formation of carbonyl compounds from UV-induced photodegradation of humic substances in natural waters: fate of riverine carbon in the sea. Limnol Oceanogr 35:1503–1515

Kirchman DL, Ducklow HW, McCarthy JJ, Garside C (1994) Biomass and nitrogen uptake by heterotrophic bacteria during the spring phytoplankton bloom in the North Atlantic Ocean. Deep Sea Res 41:879–895

Kirchman DL, Lancelot C, Fasham M, Legendre L, Radach G, Scott M (1993) Dissolved organic material in biogeochemical models of the ocean. In: Evans GT, Fasham MJR (eds) Towards a model of ocean biogeochemical processes. Series I: Global Environmental Change 10, Berlin, p 209–225

Kirchman DL, Suzuki Y, Garside C, Ducklow HW (1991) High turnover rates of dissolved organic carbon during a spring phytoplankton bloom. Nature 352:612–614

Lavín A, Díaz del Río G, Cabanas JM, Casas G (1991) Afloramiento en el noroeste de la Península Ibérica. Indices de afloramiento para el punto 43°N 11°W: periodo 1966–89. Informes Técnicos del Instituto Español de Oceanografía 41, Minist. de Agricultura Pesca y Alimentación, Madrid

Laws E (1991) Photosynthetic quotients, new production and net community production in the open ocean. Deep Sea Res 38:143–167

Lefèvre D, Denis M, Lambert CE, Miquel JC (1996) Is DOC the main source of organic matter remineralisation in the ocean water column? J Mar Syst 7:281–291

Ludwig W, Probst JP, Kempe S (1996) Predicting the oceanic input of organic carbon by continental erosion. Global Biogeochem Cycles 10:23–41

McClain CR, Chao S, Atkinson LP, Blanton JO, Castillejo F (1986) Wind-driven upwelling in the vicinity of Cape Finisterre, Spain. J Geophys Res 91:8470–8486

Mehrbach C, Culberson CH, Hawley JE, Pytkowicz RM (1973) Measurements of the apparent dissociation constant of carbonic acid in seawater at atmospheric pressure. Limnol Oceanogr 18:897–907

Meybeck M (1982) Carbon, nitrogen and phosphorus trans-

port by world rivers. Am J Sci 282:401–450
Middelburg JJ, Vlug T, Van der Nat FJWA (1993) Organic matter mineralization in marine systems. Global Planet Change 8:47–58
Millard RC, Owens WB, Fofonoff NP (1990) On the calculations of the Brunt-Väisälä frequency. Deep Sea Res 37: 167–181
Moncoiffé G (1995) The response of microbial plankton photosynthetic, respiration and growth rates to upwelling processes in the Ría de Vigo (NW Spain). PhD thesis, University of Belfast
Mopper K, Zhou X, Kieber RJ, Sirkorsky RJ, Jones RD (1991) Photochemical degradation of dissolved organic carbon and its impact on the oceanic carbon cycles. Nature 353: 60–62
Mouriño C, Fraga F (1985) Determinación de nitratos en agua de mar. Invest Pesq 49:89–96
Mouriño C, Fraga F, Fernandez F (1984) Hidrografía de la ría de Vigo 1979–1980. In: Cuadernos Area de Ciencias Marinas. Seminario Estudios Galegos 1:91–103
Murray JW, Barber RT, Bacon M, Roman MR, Feely RA (1994) Physical and biological controls on carbon cycling in the Equatorial Pacific: US JOFS EqPac process study. Science 266:58–65
Nogueira E, Pérez FF, Ríos AF (1997a) Seasonal patterns and long-term trends in an estuarine upwelling ecosystem (Ría de Vigo, NW Spain). Estuar Coast Shelf Sci 44 :285–300
Nogueira E, Pérez FF, Ríos AF (1997b) Modelling thermohaline properties in an estuarine upwelling ecosystem (Ría de Vigo: NW Spain) using Box-Jenkins transfer models. Estuar Coast Shelf Sci 44:685–702
Nogueira E, Pérez FF, Ríos AF (1997c) Modelling nutrients and chlorophyll a time-series in an estuarine upwelling ecosystem (Ría de Vigo: NW Spain) using Box-Jenkins transfer models. Estuar Coast Shelf Sci (in press)
Norrman B, Zweifel UL, Hopkinson CS Jr, Fry B (1995) Production and utilisation of dissolved organic carbon during an experimental diatom bloom. Limnol Oceanogr 40: 898–907
Odum WE, Fisher JS, Pickral JC (1979) Factors controlling the flux of particulate organic carbon from estuarine wetlands. In: Livingston RJ (ed) Ecological processes in coastal and marine systems. Plenum Press, New York, p 69–80
Pakulski JD, Benner R (1994) Abundance and distribution of carbohydrates in the ocean. Limnol Oceanogr 39:930–940
Pazos Y, Figueiras FG, Álvarez-Salgado XA, Rosón G (1995) The control of succession in red tide species in the Ría de Arousa (NW Spain) by upwelling and stability. In: Lassus P, Arzul G, Erad E, Gentien P, Marcaillou C (eds) Harmful algal blooms. Lavoisier, Intercept Ltd, Paris, p 645–650
Pérez FF, Álvarez-Salgado XA, Rosón G, Ríos AF (1992) Carbonic-calcium system, nutrients and total organic nitrogen in continental runoff to the Galician Rías Baixas, NW Spain. Oceanol Acta 15:595–602
Pérez FF, Fraga F (1987a) A precise and rapid analytical procedure for alkalinity determination. Mar Chem 21. 169–182
Pérez FF, Fraga F (1987b) The pH measurements in seawater on NBS scale. Mar Chem 21:315–327
Prego R (1993a) General aspect of carbon biogeochemistry in the ría of Vigo, north-western Spain. Geochim Cosmochim Acta 57:2041–2052
Prego R (1993b) Biogeochemical pathways of phosphate in a Galician Ría (North-Western Iberian peninsula). Estuar Coast Shelf Sci 37:437–451
Prego R (1994) Nitrogen interchanges generated by biogeochemical processes in a Galician ría. Mar Chem 45: 167–176
Prego R, Fraga F (1992) A simple model to calculate the residual flows in a Spanish ría. Hydrographic consequences in the Ría of Vigo. Estuar Coast Shelf Sci 34:603–615
Prego R, Fraga F, Ríos AF (1990) Water interchange between the Ría of Vigo and the coastal shelf. Scientia Mar 54: 95–100
Ríos AF (1992) El fitoplancton en la Ría de Vigo y sus condiciones ambientales. PhD thesis, University of Santiago
Ríos AF, Nombela MA, Pérez FF, Rosón G, Fraga F (1992) Calculation of runoff to an estuary. Ría de Vigo. Scientia Mar 56:29–33
Rosón G, Álvarez-Salgado XA, Pérez FF (1997) A non-steady state box model to determine residual flows in a partially mixed estuary based on both thermohaline properties. Estuar Coast Shelf Sci 44:249–262
Rosón G, Pérez FF, Álvarez-Salgado XA, Figueiras FG (1995) Variation of both thermohaline and chemical properties in an estuarine upwelling ecosystem: Ría de Arousa. I. Time evolution. Estuar Coast Shelf Sci 41:195–213
Rosón G, Pérez FF, Álvarez-Salgado XA, Ríos AF (1991) Flujos de los aportes de agua continental a la Ría de Arosa. Scientia Mar 55:583–589
Sambrotto RN, Savidge G, Robinson C, Boyd P, Takahashi T, Karl DM, Langdon C, Chipman D, Marra J, Codispoti L (1993) Elevated consumption of carbon relative to nitrogen in the surface ocean. Nature 363:248–250
Sokal RR, Rohlf FJ (1995) Biometry. Freeman and Co, New York
Takahashi T, Olafsson J, Goddard JG, Chipman DW, Sutherland SC (1993) Seasonal variation of CO_2 and nutrients in the high-latitude surface oceans: a comparative study. Global Biogeochem Cycles 7:843–878
Tenore KR and 18 co-authors (1995) Fisheries and oceanography off Galicia, NW Spain: mesoscale spatial and temporal changes in physical processes and resultant patterns of biological productivity. J Geophys Res 100:10943–10966
Thomas C, Cauwet G, Minster JF (1995) Dissolved organic carbon in the equatorial Atlantic Ocean. Mar Chem 49: 155–169
UNESCO (1985) The international system of units (SI) in oceanography. UNESCO Tech Pap Mar Sci 45
Walsh JJ (1991) Importance of continental margins in the marine biogeochemical cycling of carbon and nitrogen. Nature 350:53–55
Wetzel RG, Hatcher PG, Bianchi TS (1995) Natural photolysis by ultraviolet irradiance of recalcitrant dissolved organic matter to simple substrates for rapid bacterial metabolism. Limnol Oceanogr 40:1369–1380
Williams PJleB (1995) Evidence for the seasonal accumulation of carbon-rich dissolved organic material, its scale in comparison with changes in particulate material and the consequential effect on net C/N assimilation ratios. Mar Chem 51:17–29
Wollast R (1991) The coastal carbon cycle: fluxes, sources and sinks. In: Mantoura RFC, Martin JM, Wollast R (eds) Ocean margin processes in global change. J Willey & Sons, Chichester, p 365–382
Wollast R (1993) Interactions of carbon and nitrogen cycles in the coastal zone. In: Wollast R, Mackenzie FT, Chou L

(eds) Interactions of C, N, P and S biogeochemical cycles and global change. Springer-Verlag, Berlin, p 195–210
Wooster WS, Bakun A, McClain DR (1976) The seasonal upwelling cycle along the eastern boundary of the North Atlantic. J Mar Res 34:131–141
Zimmerman RC, Kremer JN, Dugdale RC (1987) Acceleration of nutrient uptake by phytoplankton in a coastal upwelling ecosystem: a modelling analysis. Limnol Oceanogr 32:359–367
Zweifel UL, Wikner J, Hagström Å (1995) Dynamics of dissolved organic carbon in a coastal ecosystem. Limnol Oceanogr 40:299–305

Editorial responsibility: Otto Kinne, Oldendorf/Luhe, Germany

Submitted: April 4, 1997; Accepted: July 21, 1997
Proofs received from author(s): September 25, 1997